



HAL
open science

Functional characterization of a plastidial cytochrome b5-fused Δ 4-desaturase from *Ostreococcus tauri* in higher plants

M Miklaszewska, Rodrigo Enrique Gomez, Pierre van Delft, M Le Guédard, C Chambaud, Cécile Mirande-Bret, L Fouillen, F Corellou, F Domergue

► To cite this version:

M Miklaszewska, Rodrigo Enrique Gomez, Pierre van Delft, M Le Guédard, C Chambaud, et al.. Functional characterization of a plastidial cytochrome b5-fused Δ 4-desaturase from *Ostreococcus tauri* in higher plants. *Biochimie*, In press, 239, pp.73-85. 10.1016/j.biochi.2025.08.019 . hal-05262002

HAL Id: hal-05262002

<https://hal.science/hal-05262002v1>

Submitted on 15 Sep 2025

HAL is a multi-disciplinary open access archive for the deposit and dissemination of scientific research documents, whether they are published or not. The documents may come from teaching and research institutions in France or abroad, or from public or private research centers.

L'archive ouverte pluridisciplinaire **HAL**, est destinée au dépôt et à la diffusion de documents scientifiques de niveau recherche, publiés ou non, émanant des établissements d'enseignement et de recherche français ou étrangers, des laboratoires publics ou privés.



HAL Authorization



Contents lists available at ScienceDirect

Biochimie

journal homepage: www.elsevier.com/locate/biochi

Functional characterization of a plastidial cytochrome b5-fused $\Delta 4$ -desaturase from *Ostreococcus tauri* in higher plants

M. Miklaszewska^{a,b,c}, R.E. Gomez^a, P. Van Delft^a, M. Le Guédard^a, C. Chambaud^a, C. Mirande-Bret^a, L. Fouillen^a, F. Corellou^{a,1}, F. Domergue^{a,*,2}

^a Univ. Bordeaux, CNRS, LBM, UMR 5200, Villenave d'Ornon, F-33140 France

^b Department of Plant Experimental Biology and Biotechnology, University of Gdańsk, Wita Stwosza 59, Gdańsk, 80-308, Poland

^c Bielefeld University, Faculty of Biology, Center for Biotechnology (CeBiTec), Universitätsstrasse 27, 33615, Bielefeld, Germany

ARTICLE INFO

Article history:

Received 2 May 2025

Received in revised form

12 August 2025

Accepted 31 August 2025

Available online xxx

Handling Editor: C. Forest

Keywords:

Desaturase

Hexadecatetraenoic acid

Polyunsaturated fatty acids

Heterologous expression

ABSTRACT

Marine microalgae are the primary producers of important lipids in oceanic ecosystems. In particular, they sustain the food web with omega-3 very-long-chain polyunsaturated fatty acids (n-3 PUFAs), which play a protective role against various human metabolic disorders and are thus considered highly beneficial to health. *Ostreococcus tauri* is a marine pico-eukaryote that contains high levels of several n-3 PUFAs, including docosahexaenoic acid (22:6n3; DHA), octadecapentaenoic acid (18:5n3, OPA), and hexadecatetraenoic acid (16:4n3), each with a distinct distribution. While DHA and OPA are restricted to microsomal and plastidial lipids, respectively, 16:4n3 is found in galactolipids as well as in betaine and neutral lipids. The genome of *O. tauri* contains 14 genes encoding fatty acid desaturases. In this study, we characterized the enzyme encoded by *OT_ostta13g01550* (*Ot13bDES*) as a plastidial cytochrome b5-fused delta-4 desaturase involved in 16:4n3 biosynthesis. Transient heterologous expression of *Ot13bDES* in *Nicotiana benthamiana* led to the production of 16:4n3 and 16:3n6, but failed to produce 18:5n3 when *Ot13bDES* was coexpressed with plastidial $\Delta 6$ -desaturases, suggesting *Ot13bDES* has a strict $\Delta 4$ regioselectivity. Lipidomic analyses of stable transgenic Arabidopsis lines further showed a nearly 100 % conversion rate of 16:3n3 to 16:4n3 in the best-performing lines, demonstrating that *Ot13bDES* has a very high catalytic activity. Additionally, 16:4n3 was predominantly localized to monogalactosyldiacylglycerol (MGDG). This study provides the first functional characterization of a plastidial cytochrome b5-fused delta-4 desaturase through heterologous expression in higher plants.

© 2025 Published by Elsevier B.V.

1. Introduction

Marine microalgae play a pivotal role in oceanic ecosystems as primary producers of essential lipids. In particular, they fuel the food web with long-chain omega-3 polyunsaturated fatty acids (n-

3 PUFAs). These compounds are highly valued for their health benefits, driving significant research into their metabolism. Consequently, the biosynthetic pathways of key PUFAs such as eicosapentaenoic acid (EPA; 20:5n3 Δ 5,8,11,14,17) and DHA (22:6n3 Δ 4,7,10,13,16,19) have been extensively studied in various

Abbreviations: ACP, Acyl Carrier Protein; CoA, coenzyme A; cTP, chloroplast targeting peptide; DAG, diacylglycerol; DES, Desaturase; DGDG, DiGalactosylDiacylGlycerol; DGTS, DiacylGlycerolTrimethylthio-Serine; DGTA, DiacylGlycerolhydroxymethylTrimethyl- β -Alanine; DHA, DocosaHexaenoic Acid; EPA, EicosaPentaenoic Acid; FAD, Fatty Acid Desaturase; FAMES, Fatty Acid Methyl Esters; FW, fresh weight; GC, Gas Chromatography; LC-MS, Liquid Chromatography-Mass Spectrometry; MGDG, MonoGalactosylDiacylGlycerol; OPA, OctadecaPentaenoic Acid; PC, PhosphatidylCholine; PDPT, PhosphatidylDimethylPropaneThiol; PE, PhosphatidylEthanolamine; PG, PhosphatidylGlycerol; PGTS, Post-Transcriptional Gene Silencing; PI, PhosphatidylInositol; PS, PhosphatidylSerine; PUFAs, PolyUnsaturated Fatty Acids; TAG, triacylglycerol; TLC, thin-layer chromatography; YFP, Yellow Fluorescent Protein.

* Corresponding author. Laboratoire de Biogenèse Membranaire, UMR5200, CNRS-Université de Bordeaux, Bâtiment A3, INRAE Bordeaux Aquitaine, 71 Avenue Edouard Bourloux, CS20032, Villenave d'Ornon, F-33140, France.

E-mail address: frederic.domergue@u-bordeaux.fr (F. Domergue).

¹ Present address: LPCV, CEA, INRAE, CNRS, Université Grenoble Alpes, UMR 5168, F-38000, Grenoble France.

² The author responsible for distribution of materials integral to the findings presented in this article in accordance with the policy described in the Instructions for Authors is Frédéric DOMERGUE (frederic.domergue@u-bordeaux.fr)

<https://doi.org/10.1016/j.biochi.2025.08.019>

0300-9084/© 2025 Published by Elsevier B.V.

Please cite this article as: M. Miklaszewska, R.E. Gomez, P. Van Delft *et al.*, Functional characterization of a plastidial cytochrome b5-fused $\Delta 4$ -desaturase from *Ostreococcus tauri* in higher plants, *Biochimie*, <https://doi.org/10.1016/j.biochi.2025.08.019>

algae [1]. While a few species developed an anaerobic polyketide synthase-based pathway for PUFA biosynthesis, most algae produce them *via* the classical aerobic desaturation/elongation pathway [1]. This pathway starts in the plastid, where 18:0, produced by the fatty acid synthase, is converted through the action of three successive desaturases to 18:3n3 Δ 9,12,15. This fatty acid is then exported to the endoplasmic reticulum, where front-end desaturases and elongases further convert it to EPA and/or DHA. Recently, it was found that an aerobic and an anaerobic pathway, producing OPA and DHA, respectively, coexist in the unicellular marine alga *Emiliania huxleyi* [2].

Fatty acid desaturases are critical for PUFA metabolism since they introduce carbon-carbon double bonds in fatty acyl chains. These oxygenases remove two hydrogen atoms using an electron donor for the oxidative process and activated oxygen as a co-substrate, yielding a molecule of water as a co-product [3]. Front-end desaturases insert the new double bond between the carboxyl end of the acyl chain and a pre-existing double bond, and they possess an N-terminal cytochrome *b5*-like domain (except in bacteria), which is essential for electron transfer [4]. Front-end desaturases from algae, plants, fungi, and animals are mostly located in the endoplasmic reticulum, and share the same structure and topology, possessing three highly characteristic histidine motifs important for the positioning of the di-iron catalytic center [5]. Despite having very similar structures, front-end desaturases with different regioselectivities (Δ 4, 5, 6, or 8) have been characterized in PUFA-producing organisms [4].

The unusual PUFA hexadecatetraenoic acid (16:4n3 Δ 4,7,10,13) has been found in high proportions in marine microalgae belonging to the Chlorophyceae and Mamiellophyceae (formerly Prasinophyceae; [6]) classes [7–10]. Recently, 16:4n3 has been proposed as a hallmark of the chlorophyte lineage, although it has been detected in some diatoms as well [11]. This PUFA is also found in the green seaweed *Ulva pertusa*, which serves as raw material for its purification as an analytical standard [12,13]. Its presence was also reported in the edible brown alga *Undaria pinnatifida* (also known as Wakame; [14]), in the star-shaped dinoflagellate *Asterodinium gracile* [15], in the green alga *Chlamydomonas reinhardtii* [16], as well as in the flagellated microalga *Euglena gracilis* [17]. Detailed lipid analysis of the last three species indicated that 16:4n3 is highly enriched at the *sn*-2 position of thylakoid galactolipids, especially MGDG [15,17,18]. For example, in *C. reinhardtii*, 16:4n3 constitutes approximately 13 % of total acyl chains, but accounts for as much as 67 mol% of the fatty acids at the MGDG *sn*-2 position, while digalactosyldiacylglycerol (DGDG) and diacylglyceryltrimethylhomo-Serine (DGTS) only contain 2 mol% of 16:4n3 [18]. Consequently, MGDG 34:7 (18:3n3/16:4n3) represents the predominant molecular species in *C. reinhardtii* (67 % of all MGDGs; [16]). In *Asterodinium gracile*, MGDG 34:9 (18:5n3/16:4n3) was reported to account for 65 % of all MGDGs [15], while in *O. tauri*, MGDG 34:8 (18:4n3/16:4n3) and MGDG 34:7 (18:3n3/16:4n3) are the most abundant (40 % and 26 %, respectively; [19]). The very specific location of 16:4n3 in these algae mirrors the situation of 16:3n3 Δ 7,10,13 in higher plants, in which 16:3n3 is nearly exclusively found at the *sn*-2 position of MGDG [20]. In higher plants, the successive activities of three Fatty Acid Desaturases (FAD5, FAD6, and FAD7 or 8) were shown to be responsible for converting 16:0 into 16:3n3 at the *sn*-2 position of MGDG *via* the so-called prokaryotic pathway [21]. Similarly, 16:3n3 biosynthesis in *C. reinhardtii* involves three plastidial fatty acid desaturases (CrFAD5, CrFAD6, and CrFAD7), which convert 16:0 at the *sn*-2 position of MGDG into 16:3n3 [16]. The final desaturation step, leading to 16:4n3, is proposed to rely on the unusual Cr Δ 4FAD desaturase identified by Zäuner et al. [22]. While all plastidial desaturases depend on ferredoxin, ferredoxin reductase,

and NADPH for electron transport, Cr Δ 4FAD was the first discovered plastid-located desaturase that contains the N-terminal cytochrome *b5* domain usually found in microsomal front-end desaturases [22]. Interestingly, misregulation of Cr Δ 4FAD expression in knockdown and overexpression *Chlamydomonas* lines did not affect MGDG 16:4n3 levels, but slightly impacted the overall 16:4n3 level by altering the MGDG to DGDG ratio. This result suggests a link between 16:4n3 availability and MGDG abundance, as well as the predominant role of Cr Δ 4FAD in galactolipid homeostasis in *C. reinhardtii* [22]. In addition, detection of 16:4n3-derived oxylipins in *Chlamydomonas debaryana* suggests that this fatty acid is a potential precursor of several important signalling molecules [23]. Finally, it should be pointed out that the presence of a 16:4 isomer, 16:4n1 Δ 6,9,12,15, was described in Bacillariophyceae [9,10], and its biosynthesis tentatively elucidated in *Phaeodactylum tricornutum* [24,25].

Ostreococcus tauri, a marine pico-eukaryote belonging to the Mamiellophyceae (Classis nova), contains 16:4n3 as the most abundant PUFA, representing close to 20 % of total fatty acids [19]. *O. tauri* displays a very distinctive PUFA distribution with very-long-chain PUFAs, such as DHA, being exclusively present in extraplastidic lipids (*i.e.*, the betaine lipid diacylglycerylhydroxymethyltrimethyl- β -alanine (DGTA), and the peculiar phosphosulfolipid, phosphatidyltrimethylpropanethiol (PDPT)), while shorter *n*-3 PUFAs (C16 and C18) are highly abundant in plastidial galactolipids, with 18:5n3 occurring only in galactolipids. Noteworthy, 16:4n3 is the most abundant PUFA in MGDG, accounting for 40 % of its total fatty acids, although it is restricted to the *sn*-2 position. 16:4n3 is also present in all other lipid classes, particularly in DGTA and neutral lipids (di- and triacylglycerol, DAG and TAG), where it constitutes 15–20 % of total fatty acids [19]. This suggests that in *O. tauri*, 16:4n3 might be converted from 16:3n3 in MGDG and subsequently exported to extraplastidial lipids [26]. Interestingly, two plastid-localized front-end desaturases were recently reported in *O. tauri*, namely Ot05DES and Ot10DES. These enzymes were characterized as Δ 6-desaturases involved in the regulation of the C18-PUFA plastidial and microsomal pools [26].

The genome of *O. tauri* contains 14 genes encoding putative fatty acid desaturases, half of which contain an N-terminal cytochrome *b5* fused domain [26]. While five of these have already been characterized [26–29], none has been shown to be involved in 16:4n3 biosynthesis. In this study, we report the identification of the enzyme encoded by *OT_ostta13g01550* (CEG00114.1) as a plastidial cytochrome *b5*-fused delta-4 desaturase responsible for 16:4n3 biosynthesis. Its activity and impact on PUFA metabolism were studied by functional characterization through transient and stable heterologous expression in *Nicotiana benthamiana* and *Arabidopsis thaliana* lines, respectively, followed by detailed lipidomic analyses.

2. Methods

2.1. Biological material and growth conditions

Ostreococcus tauri (clonal isolate from OtH95), *Saccharomyces cerevisiae* (strain InvSc1), *Agrobacterium tumefaciens* (strain GV3101), and *Nicotiana benthamiana* plants were grown as previously described [26]. *Arabidopsis thaliana* (ecotype Columbia-0) was used in all experiments and grown under controlled conditions as previously described [30].

2.2. Cloning of *O. tauri* desaturases

OtDES coding sequences were amplified from cDNA using Q5® Polymerase and the primers indicated in Table S1. The

corresponding PCR fragments were cloned into pDONR™221 ENTRY vector by the GATEWAY® recombinational cloning technology using the *attB* × *attP* (BP) recombination sites. Fragments containing ORF sequences were subsequently transferred into pVT102-U-GW (yeast expression), pK7W2G2D (plant overexpression), or pK7YWG2 (plant overexpression and subcellular localization) DESTINATION vectors by LR cloning.

2.3. Sequence analyses

Amino acid sequence alignments were obtained using the MEGA11 program (gap opening 10, gap extension 0.05), and the phylogenetic tree was constructed by the neighbor-joining method using Tree View. Evolutionary analyses were conducted in MEGA11 [31], and the phylogenetic tree was generated using the Maximum Likelihood method and JTT matrix-based model [32]. Initial tree(s) for the heuristic search were obtained automatically by applying the Neighbor-Join and BioNJ algorithms to a matrix of pairwise distances estimated using the JTT model, and then selecting the topology with the superior log likelihood value. Sequence logos for Histidine boxes were drawn using WebLogo [33].

2.4. Heterologous expression in *Saccharomyces cerevisiae*

S. cerevisiae strain INVSC1 (Invitrogen) was transformed with the different DNA constructs using a PEG/lithium acetate protocol [34], and transformants were selected on minimal agar plates lacking uracil. Transgenic yeasts expressing desaturase genes were cultivated in minimal medium lacking uracil at 30 °C, and exogenous fatty acids (22:5n3) were supplied at a final concentration of 500 μM 24 h after starting the culture. Cells were harvested by centrifugation (2000g for 5 min) 4 days later, and cell pellets were directly used for fatty acid analysis.

2.5. Transient expression in *Nicotiana benthamiana*

A. tumefaciens strains that have been transformed with the different DNA constructs (using a standard protocol for chemocompetent cell transformation) were grown overnight. The cultures were diluted to an OD₆₀₀ of 0.1 and grown to a final OD₆₀₀ of 0.6–0.8. The cells were harvested by centrifugation (2000g for 5 min), re-suspended in 5 mL sterilized H₂O, and infiltration solutions were prepared. To minimize plant post-transcriptional gene silencing (PTGS), each solution contained the p19 strain (final OD₆₀₀ of 0.1). Strains containing our constructs of interest had a final OD₆₀₀ of 0.3, 0.15, or 0.1 when expressing one, two or three genes, respectively. The abaxial sides of *N. benthamiana* leaves from five-week-old plants were infiltrated, and plants were used for lipid analysis 5 days post-agroinfiltration.

2.6. Stable expression in *Arabidopsis thaliana*

A. tumefaciens strains transformed with the different DNA constructs were used to generate stably transformed *Arabidopsis* plants using the floral-dip transformation method [35]. Representative transgenic lines were selected according to their leaf fatty acid profiles, and T3 and T4 generations were used in all experiments.

2.7. Lipid extraction and analysis

For total fatty acyl-chain profiling, samples (leaf discs or yeast cell pellets) were directly transmethylated with 1 mL of methanol containing 2.5 % (v/v) H₂SO₄ for 1 h at 85 °C. After cooling, 1 mL of

hexane and 1 mL of NaCl (2.5 %, w/v) were added, and samples were vigorously shaken and centrifuged (2000g for 5 min). The hexane phase containing fatty acid methyl esters (FAMES) was then directly used for gas chromatography (GC) analysis.

Arabidopsis lipid extracts were prepared from six-week-old leaves (250–500 mg fresh weight; FW) using organic solvents that all contained 0.01 % butylhydroxytoluene as an antioxidant. Harvested leaves were weighted, immediately frozen with liquid nitrogen, broken into pieces, and stored at –20 °C until further use. Lipids were first extracted with hot isopropanol (2.5 mL, 30 min, 85 °C) for phospholipase D inhibition, and then twice with 2:1 (v/v) CHCl₃:CH₃OH (2.5 mL, 1 h, room temperature). Two mL NaCl 2.5 % (w/v) were added to the combined organic extracts, and samples were vigorously shaken and centrifuged (2000g for 5 min) for phase separation. The lower organic phase containing lipids was collected, evaporated under a stream of nitrogen, and the total lipid extracts were resuspended in 1:1 (v/v) CHCl₃:CH₃OH (final concentration 100 mg FW/ml). For thin-layer chromatography (TLC) separation, total lipid extracts (500 μl) were loaded on HPTLC Silica Gel 60 plates (Merck), and polar lipids were separated using chloroform/methyl acetate/1-propanol/methanol/KCl 0.25 % (10:10:10:4:3.6, v/v/v/v/v) as the solvent system. The different lipid subclasses were then scraped from the TLC plate, and their fatty acyl-chain compositions analysed by GC. For determining relative glycerolipid compositions, transmethylation was done in the presence of 5 μg of heptadecanoic acid, which was then used to normalize the quantity of total acyl-chains present in each lipid subclass (the total acyl-chains present in all subclasses corresponding to 100 %).

2.8. GC and LC-MS analyses

Separation and quantification of fatty acyl chains were routinely performed by gas chromatography (7890A GC system; Agilent Technologies) on a 15 m × 0.53 mm × 1 μm DB-Wax column (Agilent Technologies) with flame ionization detection. The oven temperature was programmed for 1 min at 150 °C, followed by a 5 °C min⁻¹ ramp to 230 °C, and maintained at this temperature for 7 min (total run time, 24 min). Fatty acid identification was performed by gas chromatography/mass spectrometry using an Agilent 7890B gas chromatograph equipped with a 60 m × 0.25 mm × 0.25 μm DB-23 column (Agilent Technologies) and an Agilent 5975 mass spectrometric detector (70 eV, mass-to-charge ratio 50–750), with helium (0.8 ml/min) as carrier gas. The oven temperature was programmed for 1 min at 80 °C, followed by a 65 °C min⁻¹ ramp to 130 °C, a 5 °C min⁻¹ ramp to 230 °C, and maintained at this temperature for 4.2 (total run time, 30 min).

For Liquid Chromatography-Mass spectrometry (LC-MS) molecular profiling, lipid extracts were dissolved in 100 μL of eluent A (methanol/water 6:4 (v/v) with 5 mM ammonium formate and 0.1 % (v/v) formic acid) containing PE 17:0/17:0 (Avanti Polar Lipids) as a synthetic internal lipid standard. LC-MS (multiple reaction monitoring mode) analyses were performed using a QTRAP 5500 (Sciex) mass spectrometer coupled to a 1290 Infinity II (Agilent Technologies) liquid chromatography system. Mass spectrometry analyses were performed in negative and positive modes. MS instrument parameters were as follows: Turbo V source temperature was set at 400 °C; curtain gas (nitrogen) was set at 35 psi; the nebulizing and drying gas (both nitrogen) were set at 40 psi, and the ion spray voltage was set at +5500 V or –4500 V (positive and negative mode respectively); depending on the lipid classes, the declustering potential was set at +35, +90V, –35V, –50V or –70V, and the collision energy (the collision gas was also nitrogen) was set at +19eV, +37 eV, –43eV, –50eV, –55eV or –60eV. Reverse-phase separation was

performed at 40 °C on a Supercolsil ABZ plus 2.1 × 100 mm column with 120 Å pore size and 3-µm particles (Supelco). The gradient elution program was as follows: 0 min, 20 % of eluent B (isopropanol/methanol 8/2 (v/v) with 5 mM ammonium formate and 0.1 % (v/v) formic acid); 11 min, 50 % of eluent B; 60 min, 85 % of eluent B. The flow rate was set at 0.20 mL/min, and 20 µL sample volumes were injected. The areas of LC peaks were determined using MultiQuant software (version 2.1; ABSciex) for relative molecular lipid quantification.

2.9. Confocal microscopy

Arabidopsis leaves were observed using a Zeiss LSM880 confocal microscope equipped with a plan-apochromat 63X, 1.4 numerical aperture objective, and a 488 nm laser at 3.5 % power. The signal from Yellow Fluorescent Protein (YFP) was collected at 517–561 nm, and chlorophyll autofluorescence at 676–723 nm.

2.10. Statistical analysis

All statistical analyses in this study were performed using R software (version 4.3.1) through RStudio (2023.06.1 + 524). Group comparisons between each overexpression condition and the corresponding control were conducted using the Kruskal-Wallis rank sum test with Dunn post-hoc analysis. These non-parametric methods were selected due to the limited number of biological replicates (3–10) and/or the violation of assumptions underlying parametric tests (*i.e.* normality of distributions and homogeneity of variances). A p-value below 0.05 was considered statistically significant.

3. Results

3.1. Sequence and phylogenetic analysis of *O. tauri* Δ4-desaturases

In a previous study [26], we identified seven front-end desaturases in the genome of *O. tauri*, completed their full-length sequences based on available RNAseq data (*de novo* contigation), and unveiled frequent N-terminal extensions in their sequences that were positively confirmed by PCR amplification on cDNA. Among them, two novel plastidic Δ6/Δ8 desaturases, Ot05DES and Ot10DES, as well as the sphingolipid Δ8-desaturase, have now been functionally characterized [26,29]. The present study focused on another unusual cytochrome-b5 fused fatty acid desaturase, encoded by *OT_ostta13g01550* and thereafter referred to as *Ot13bDES*, which was putatively annotated as a plastidial Δ4-desaturase homologue [26].

As shown in Fig. 1A, Ot13bDES is a 534 amino acid (aa) long protein and contains 2 pfam domains, a cytochrome-b5 domain with the HPGG motif (aa 96–170), and a desaturase domain with the three characteristic His-boxes (HCANH, HQVSHH, and QVEHH; aa 228–493). The hydrophobicity plot revealed four transmembrane domains responsible for membrane anchoring. Interestingly, the PredAlgo prediction software [36] predicted the presence of a 51 aa-long chloroplast targeting peptide (cTP) with a score of 2.51 (of 5). A shorter (518 aa) version starting from the downstream methionine was predicted to have a 37 aa-long cTP with a score of 3.14.

To gain insights into Ot13bDES potential activity, we first constructed a phylogenetic neighbor-joining tree using the MEGA-11 software (Fig. 1B). We used cytochrome-b5 fused desaturase sequences from various algae and higher plants, including all seven cytochrome-b5 fused desaturases from *O. tauri*, as well as the sphingolipid Δ4-desaturase from Arabidopsis (encoded by *At4g04930*), which does not contain such a domain, for rooting.

The resulting tree showed two major clades, a minor one with microsomal acyl-CoA Δ6-desaturases specific to Mamiellophyceae species, and a major one with front-end desaturases with various specificities. In this second group, two main clusters can be distinguished: Δ4/Δ5-desaturases and Δ6/Δ8-desaturases, the latter of which includes sphingolipid Δ8-desaturases. Interestingly, Ot13bDES clustered with putative Δ4-desaturases from *Monoraphidium minutum*, *Dunaliella salina*, and *Scenedesmus* sp., as well as with the plastid-localized Δ4-desaturase from *C. reinhardtii* (CrΔ4FAD) [22]. As shown in Fig. 1B, these enzymes indeed formed a distinct branch separate from the functionally characterized microsomal Δ4/Δ5-desaturases, which is in agreement with our previous phylogenetic analysis that was restricted to front-end desaturases from *Mamiellales* [29]. Noteworthy, Ot13bDES was also close to another front-end desaturase from *O. tauri*, Ot01DES, which is highly similar (76 % identical/83 % homologous) to the functionally characterized microsomal Δ4-desaturases from *Ostreococcus lucimarinus* [28].

3.2. Functional characterization of *Ot13bDES* by heterologous expression

The presence of a putative transit peptide and the similarity of Ot13bDES to CrΔ4FAD suggested that this protein could be a plastidial Δ4-desaturase. However, the complete sequence of the putative microsomal Ot01DES (partially encoded *OT_Ostta01g00790*, see Supplemental Fig. S1A) was also predicted to contain a cTP with a score of 2.31 by PredAlgo [26]. Consequently, we first characterized the activity of both Ot13bDES and Ot01DES proteins by heterologous expression in *S. cerevisiae*. To check for microsomal Δ4-desaturase activity, yeast cultures were supplied with 22:5n3Δ7,10,13,16,19, and their fatty acid profiles were analysed by GC. While the expression of *Ot01DES* resulted in the detection of 22:6n3Δ4,7,10,13,16,19, confirming that Ot01DES is a microsomal Δ4-desaturase, no 22:6n3 could be detected in yeast cells expressing *Ot13bDES* (Supplemental Fig. S1B). To provide an accurate lipidic substrate for Δ4-desaturation by the putative plastidial Ot13bDES, we used *N. benthamiana* that contains high levels of MGDG18:3n3/16:3n3 [37]. Both the short (518 aa) and long (534 aa) versions of *Ot13bDES* were transiently expressed in *N. benthamiana* leaves, and the fatty acid profiles of the leaves were analysed by GC 5 days post-infiltration. While expression of the short version (518 aa) of *Ot13bDES* resulted in a wild-type fatty acid profile, two novel fatty acids, 16:4n3Δ4,7,10,13 and 16:3n6Δ4,7,10, were unambiguously detected upon expression of the Ot13bDES long (534 aa) version (Fig. 2A–C; Supplemental Fig. S2). 16:4n3Δ4,7,10,13 and 16:3n6Δ4,7,10 comprised 5.73 mol % and 0.8 mol% of the total fatty acids, respectively. Meanwhile, the concentrations of their precursors, 16:3n3Δ7,10,13 and 16:2n6Δ7,10, decreased to 1.39 mol% (6.13 mol% in the control) and 0.83 mol% (2.72 mol% in the control), respectively (Fig. 2B). Globally, Δ4 fatty acids accounted for 6.53 mol% of the total fatty acids (Fig. 2C).

In a previous study [19], we reported that *O. tauri* has the capacity to produce a peculiar fatty acid 18:5n3Δ3,6,9,12,15. 18:5n3 was found as a hallmark of galactolipids (plastidic lipids) and was assumed to be derived from 18:4n3Δ6,9,12,15 through the activity of a previously unidentified Δ3 desaturase. In agreement with this hypothesis, we recently characterized the two plastidic Δ6-DES from *O. tauri* (Ot05DES and Ot10DES), and showed that their expression in *N. benthamiana* resulted in the accumulation in plastidic lipids of high levels of the Δ6-desaturation products, especially 18:4n3 [26]. As heterodimerization of closely related desaturases and desaturase bifunctionality have both been reported, we wanted to investigate whether Ot13bDES could display

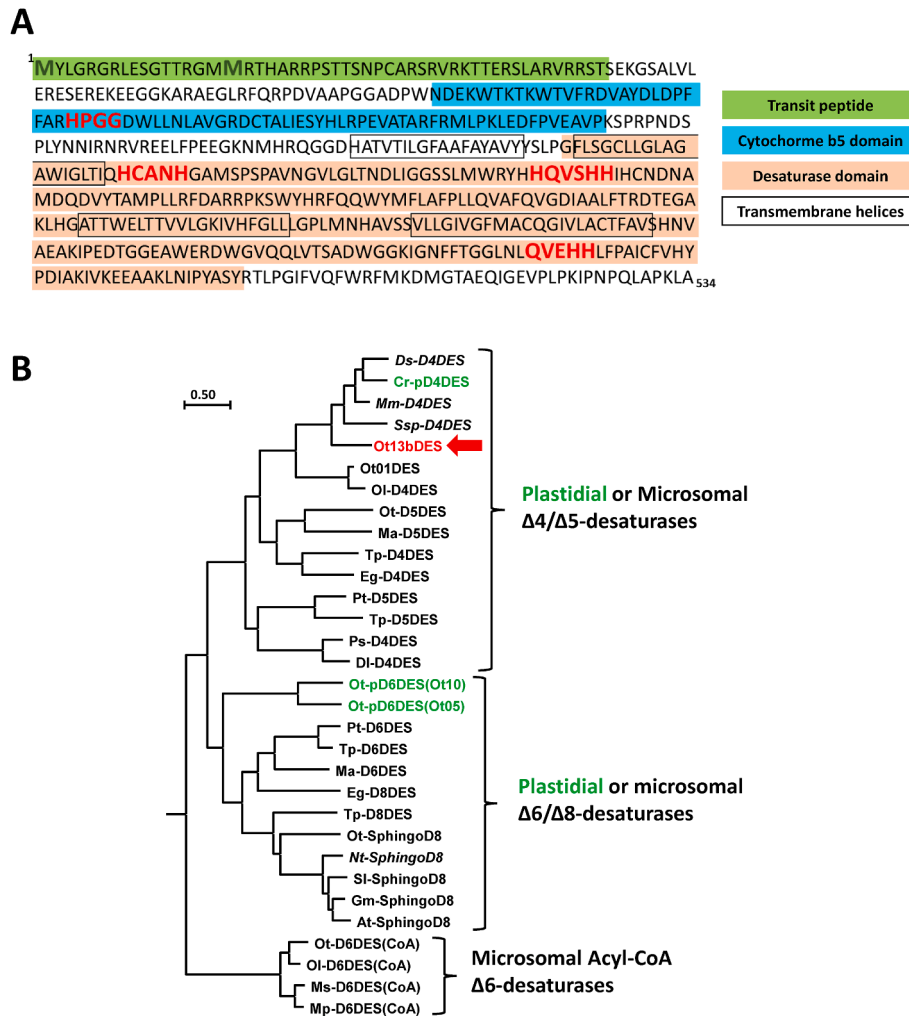


Fig. 1. Ot13bDES amino acid sequence analysis and phylogenetic tree with related desaturases from *O. tauri* and other species.

A: Ot13bDES amino acid sequence showing pfam domains, and putative targeting and transmembrane domains. Characteristic motifs of desaturase (i.e. the three histidine boxes) and cytochrome b5 domain (HPGG) are highlighted in red.

B: Phylogenetic tree of related desaturases with different substrate- and regioselectivities. The tree was constructed with MEGA11 and rooted with unrelated sphingolipid desaturase AtSLD4. The tree with the highest log likelihood (−29878.69) is shown. The tree is drawn to scale, with branch lengths measured in the number of substitutions per site. This analysis involved 32 amino acid sequences, and there were a total of 772 positions in the final dataset. Proteins which activities have not yet been confirmed are indicated in italics. Accession numbers and references are given in [Supplementary Table 2](#).

$\Delta 3$ -desaturase activity when co-expressed with plastidial $\Delta 6$ -desaturases in *N. benthamiana*. We therefore overexpressed the *Ot13bDES* long (534 aa) version together with each and both plastidial $\Delta 6$ -desaturases from *O. tauri* (Fig. 2D). Consistent with our previous report, the transient overexpression of *Ot05DES* or *Ot10DES* in *N. benthamiana* resulted in the production of 18:3n6 and 18:4n3 from 18:2n6 and 18:3n3, respectively, with the highest conversion observed for *Ot05DES* (Fig. 2D). Co-expression of *Ot05DES* and *Ot10DES* in *N. benthamiana* resulted in similar profiles, with high levels of $\Delta 6$ -desaturated fatty acids (Fig. 2D). Most importantly, while co-expression of *Ot13bDES* with either or both plastidial $\Delta 6$ -desaturases systematically resulted in the appearance of 16:4n3, 18:5n3 could never be detected in the fatty acid profiles of *N. benthamiana*. Altogether, our data showed that *Ot13bDES* is a plastidial $\Delta 4$ -desaturase with no $\Delta 3$ -desaturase activity.

A comparison of the three characteristic histidine-rich motifs of plastidial and microsomal $\Delta 4$ -desaturases (Supplemental Fig. S3) revealed a few specific amino acid differences in the first and

second motifs, whereas the third histidine motif showed a high degree of similarity. In particular, plastidial $\Delta 4$ -desaturases appeared to contain a cysteine positioned directly after the first histidine in the first box, and a histidine directly preceding the first histidine in the second box. However, these specific amino acid sequence features need to be confirmed by functionally characterizing additional plastidial $\Delta 4$ -desaturases.

3.3. Stable expression of *Ot13bDES* in *Arabidopsis* leaves

To gain more insights into *Ot13bDES* impact on the lipid homeostasis of higher plants, we also generated stable transgenic *Arabidopsis* lines expressing constitutively (using the CaMV 35S promoter) the *Ot13bDES* gene. Six lines with different levels of $\Delta 4$ -desaturase activity were selected for further characterization (Fig. 3). All lines produced 16:4n3 from 16:3n3, and the best-performing lines (*Ot13b*#30, 14, and 5) also produced 16:3n6 from 16:2n6 (Fig. 3A). The $\Delta 4$ -fatty acids represented from 2.1 to 13.3 % of the total fatty acids (Fig. 3B), with a $\Delta 4$ conversion rate

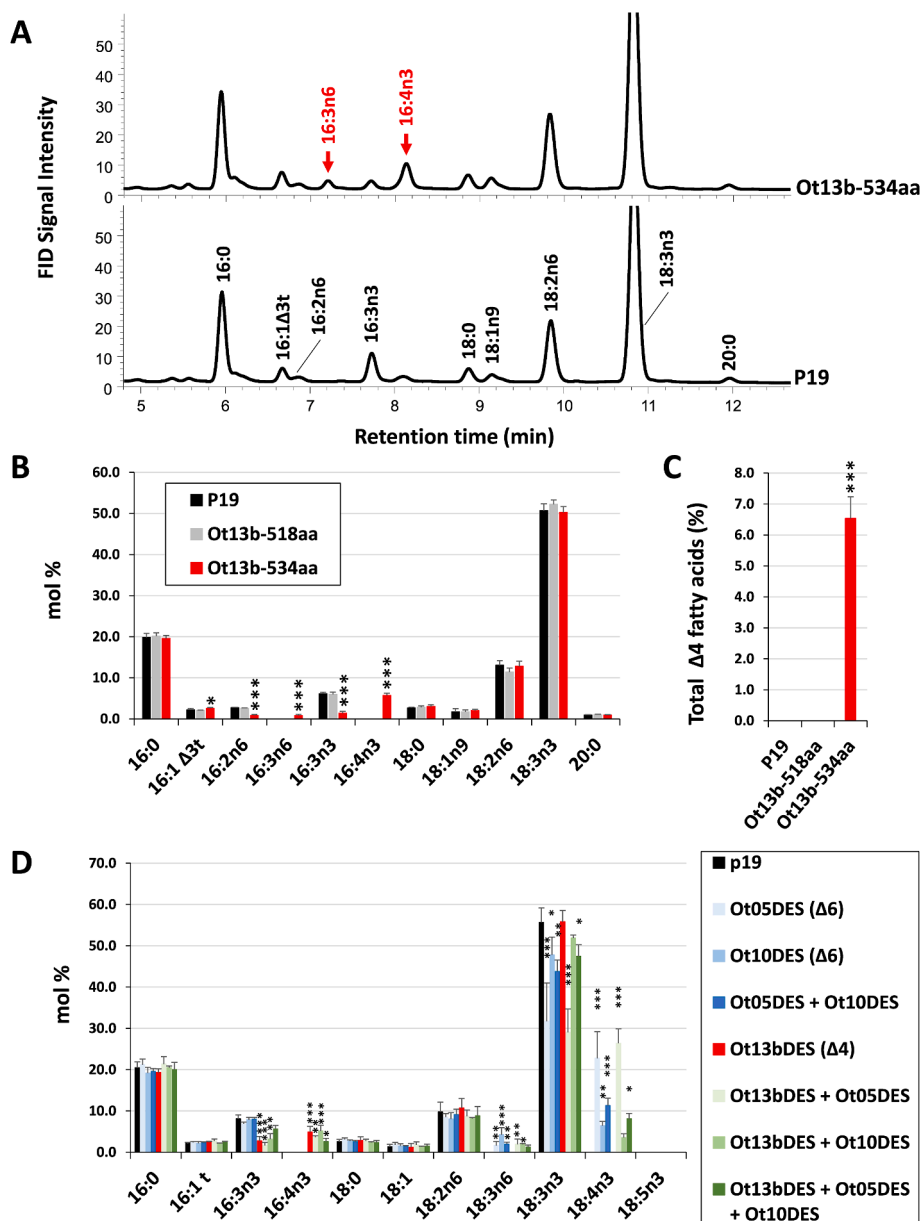


Fig. 2. Functional characterization of Ot13bDES by heterologous expression in *Nicotiana benthamiana*.

A: Fatty acid profiles of *N. benthamiana* leaves expressing Ot13bDES variants and the respective control.

B: Fatty acid composition of *N. benthamiana* leaves expressing Ot13bDES variants and the respective control.

C: Proportion of Δ4-desaturated fatty acids.

D: Fatty acid composition of *N. benthamiana* leaves expressing Ot13bDES, plastidial Δ6-desaturases (Ot05DES and Ot10DES) alone and in combination.

N. benthamiana leaves were agroinfiltrated with different molecular constructions, and their fatty acid compositions were analysed by GC 5 days post-inoculation.

The data represent means ± standard deviation of 6-8 biological replicates, and statistics were based on Kruskal-Wallis rank sum test with Dunn post-hoc analysis (*, 0.1 < p < 0.05; **, 0.05 < p < 0.01; ***p < 0.001).

ranging from 13 to 99 % (Fig. 3C). None of these lines showed any growth defects or visible differences compared to wild-type controls.

Ot13b#10, accumulating low levels of Δ4 fatty acids, and Ot13b#14 and Ot13b#5, both accumulating high levels of Δ4 fatty acids, were then further used for detailed leaf lipidomic analyses. The lipid distribution of these lines was very similar to that of the Col-0 wild-type (Fig. 4A). In agreement with the nearly specific presence of 16:3n3 in MGDG, the fatty acid composition of the other polar lipid classes was poorly affected by the introduced Δ4-desaturase activity (Supplemental Fig. S4). **Only phosphatidylcholine (PC) and DGDG contained trace amounts of 16:4n3 in**

the two lines accumulating high levels of Δ4 fatty acids (Supplemental Fig. S4). In contrast, the MGDG fatty acid composition clearly differed between Ot13bDES-overexpressing lines and the wild-type Col-0. In the line Ot13b#10, which accumulated low levels of Δ4 fatty acids, a decrease of about 4 % of 16:3n3 compared to Col-0 was accompanied by the appearance of 16:4n3, the proportion of which reached about 6 % of the total fatty acids, while 16:2n6 levels remained unaffected (Fig. 4B). In the lines accumulating high levels of Δ4 fatty acids (Ot13b#14 and Ot13b#5), 16:3n3 became barely detectable, and 16:4n3 accounted for as much as 20 % of the total fatty acids (Fig. 4B). Additionally, 16:2n6 was decreased, and 16:3n6 accumulated up to 5 % (Fig. 4B).

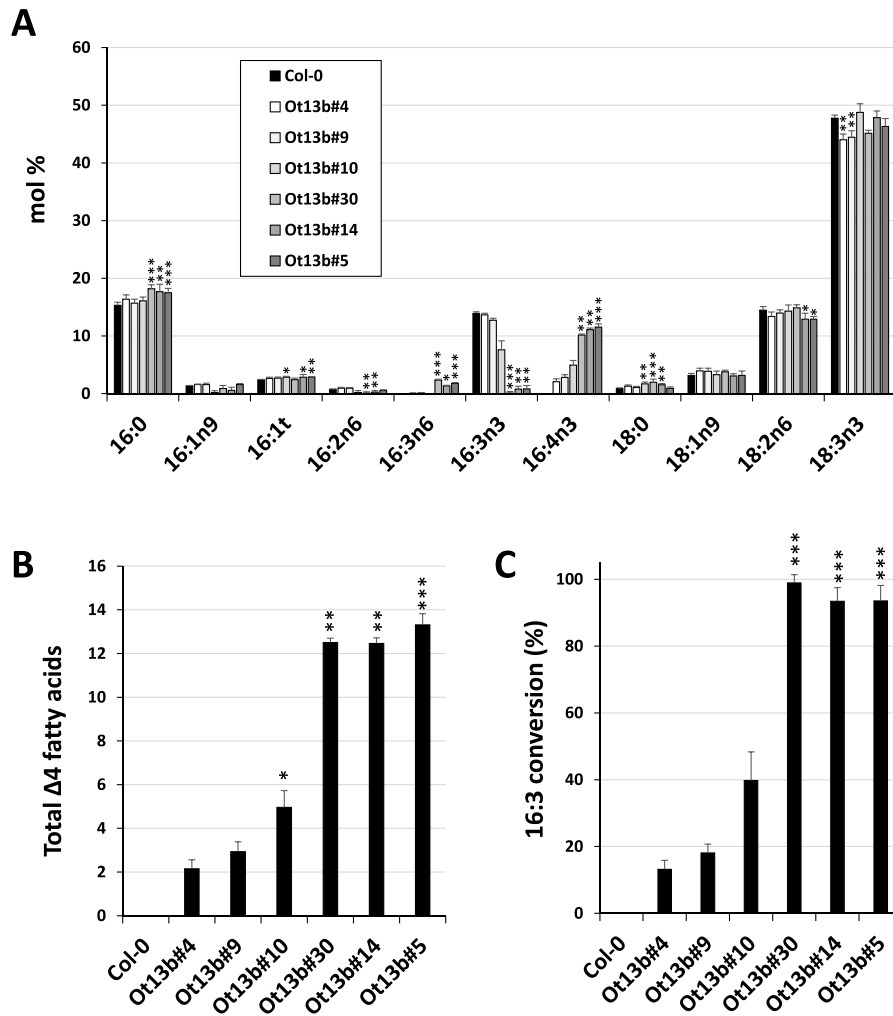


Fig. 3. Characterization of *Arabidopsis thaliana* lines overexpressing *Ot13bDES*.

A: Leaf fatty acid composition of different *Arabidopsis* lines overexpressing *Ot13bDES* and Col-0 control.

B: Proportions of $\Delta 4$ -desaturated fatty acids.

C: 16:3n3 to 16:4n3 conversion rates.

Arabidopsis lines expressing *Ot13bDES* under the control of the CaMV 35S promoter were generated, and their fatty acid compositions were analysed by GC.

The data represent means \pm standard deviation of 3–5 biological replicates, and statistics were based on Kruskal-Wallis rank sum test with Dunn post-hoc analysis (*, 0.1 < p < 0.05; **, 0.05 < p < 0.01; ***p < 0.001).

Altogether, $\Delta 4$ fatty acids accounted for as much as 25 % of the total fatty acids in MGDG (Fig. 4C). In addition, trace amounts of 18:4 were detected in MGDG in the lines accumulating high levels of $\Delta 4$ fatty acids (Fig. 4B). We confirmed that this 18:4 had a retention time very similar to that of 18:4 $\Delta 6,9,12,15$, while 18:4 $\Delta 5,9,12,15$ eluted much earlier, strongly supporting the conclusion that this compound corresponds to 18:4 $\Delta 6,9,12,15$ and not 18:4 $\Delta 4,9,12,15$ (Supplemental Fig. S5). Nevertheless, its very low abundance did not allow us to determine unambiguously the exact position of the double bonds.

To further investigate how the activity of *Ot13bDES* affected the chloroplast glycerolipid profile, lipid extracts were analysed using LC-MS molecular profiling. While the most abundant molecular species was MGDG 34:6 (18:3/16:3) in Col-0 leaves, lines accumulating high levels of $\Delta 4$ fatty acids had MGDG 34:7 (18:3/16:4) as the major species (Fig. 5A). These lines also contained minor quantities of two other new MGDG species absent in the wild type Col-0: MGDG 36:7 (18:3/18:4), and MGDG 34:8 (18:4/16:4). Conversely, the levels of MGDG 34:6 (18:3/16:3) and MGDG 34:5

(18:3/16:2) were severely reduced in these lines (Fig. 5B). In the line accumulating low levels of $\Delta 4$ fatty acids (Ot13b#10), MGDG 34:7 (18:3/16:4) was detected, but MGDG 34:6 (18:3/16:3) and MGDG 36:3 (18:3/18:3) remained the major molecular species as in Col-0. LC-MS molecular profiling also showed the presence of minor amounts of 34:7 (18:3/16:4) and 36:7 (18:3/18:4) molecular species in DGDG (Fig. 5B) and PC (Fig. 5C).

3.4. *Ot13bDES* localizes in chloroplasts

The presence of a putative transit peptide and the fact that $\Delta 4$ -activity was only observed *in planta* strongly suggested that *Ot13bDES* is a plastidial desaturase. To verify this localization, we generated transgenic *Arabidopsis* lines constitutively expressing *Ot13bDES* fused with the YFP. Two selected lines were analysed for their leaf fatty acid composition, revealing a significant accumulation of $\Delta 4$ -fatty acids (Fig. 6A and B), similar to the best-performing lines expressing *Ot13bDES* alone that were characterized above. As the presence of the YFP protein at the C-terminal

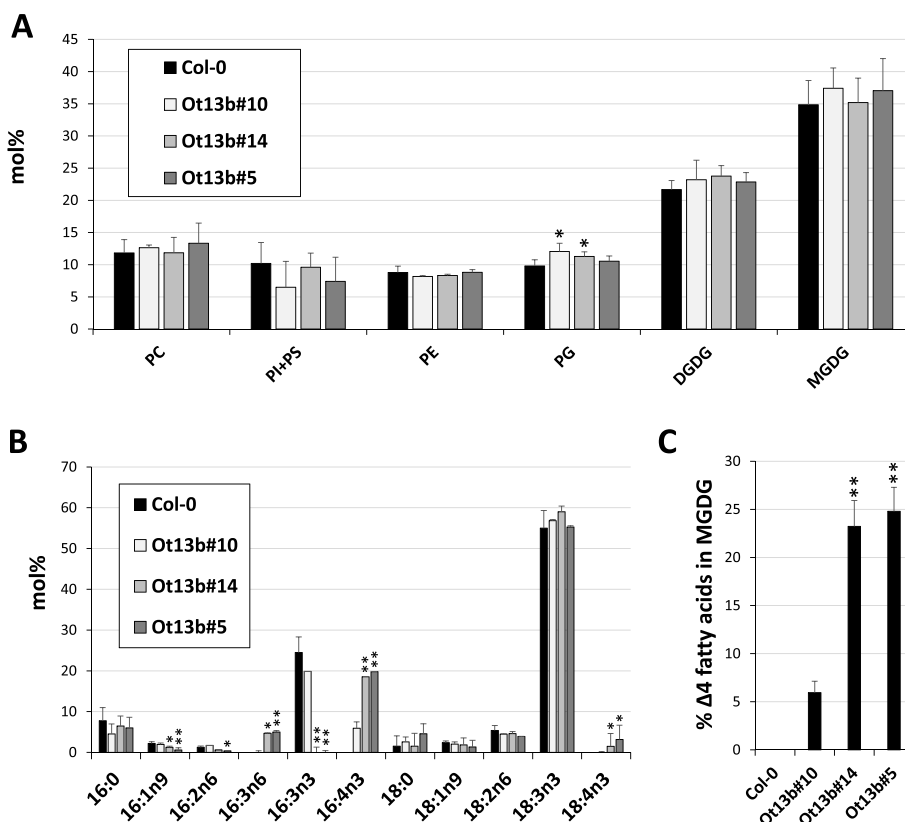


Fig. 4. Lipidomic analysis of leaves from *Arabidopsis thaliana* lines overexpressing *Ot13bDES* and Col-0 control.

A: Glycerolipid composition.

B: Fatty acid composition of MGDG.

C: Proportion of $\Delta 4$ -desaturated fatty acids in MGDG.

Lipid extracts were prepared from leaves of *Arabidopsis* lines expressing *Ot13bDES* under the control of the CaMV 35S promoter, and glycerolipids were separated by TLC. The major lipid classes (PC, Phosphatidylinositol and Phosphatidylserine (PI + PS), Phosphatidylethanolamine (PE), Phosphatidylglycerol (PG), DGDG, MGDG) were scraped off the plate, and GC analyses were used to determine their fatty acid compositions and relative contents.

The data represent means \pm standard deviation of 3–5 biological replicates, and statistics were based on Kruskal-Wallis rank sum test with Dunn post-hoc analysis (*, $0.1 < p < 0.05$; **, $0.05 < p < 0.01$; ***, $p < 0.001$).

end of *Ot13bDES* did not affect its activity, these lines were further used to check the subcellular localization of the enzyme. Confocal microscopy imaging showed a good co-localization of the YFP signal with chlorophyll. However, some YFP fluorescence was also observed outside of plastids, possibly in the endoplasmic reticulum (Fig. 6C). These non-plastidial signals could correspond to newly synthesized fusion protein on the way to the plastid, luminal cleaved YFP, or protein mislocalisation due to high over-expression levels driven by the CaMV 35S promoter, as described in Ref. [38]. Despite potential artefacts associated with over-expression, confocal imaging nevertheless supported the plastidial localization of *Ot13bDES*.

4. Discussion

A $\Delta 4$ -desaturation activity has been described in many organisms and several metabolic pathways, and different $\Delta 4$ -desaturases have already been reported. The first characterized enzyme of this type was a plastidial acyl-Acyl Carrier Protein (ACP) desaturase involved in petroselinic acid biosynthesis in the *Umbelliferae* plant family [39]. A microsomal $\Delta 4$ -desaturase responsible for the last step in DHA biosynthesis was then described in the protist *Thraustochytrium* sp. [40]. Homologs of this enzyme have ever since been characterized in many microalgae [4] and, more recently, in teleost fishes [41]. Finally, this activity also

occurs in sphingolipid metabolism, but in contrast to the activities above, with *trans*-stereospecificity. Enzymes responsible for $\Delta 4$ -desaturation of the sphingoid base have been characterized so far in a wide range of organisms from fungi to insects, plants, and animals, but no homologue has been found in *O. tauri* [29,42,43]. While acyl-ACP desaturases acting on saturated acyl chains in the plastids are always soluble, the desaturases involved in sphingolipid and PUFA metabolisms are membrane-bound and, therefore, have a completely different structure. In particular, these enzymes have a conserved membrane topology with four transmembrane helices and a di-iron catalytic center on the cytosolic side of the membrane, which is associated with the presence of the three characteristic histidine-rich motifs [44]. PUFA and sphingolipid $\Delta 4$ -desaturases share these key structural features but differ in their domain organization: while PUFA $\Delta 4$ -desaturases are classical front-end desaturases featuring an N-terminal cytochrome *b*₅-like domain, sphingolipid $\Delta 4$ -desaturases completely lack this domain.

While numerous microsomal front-end desaturases with $\Delta 4$ -, $\Delta 5$ -, $\Delta 6$ - or $\Delta 8$ -regioselectivity have been characterized to date in many different organisms [4], plastidial front-end desaturases represent a relatively new class of enzymes that remain largely unexplored. Indeed, only three enzymes of this type have been studied to date, all of them from algal species. Zäuner et al. [22] first identified a putative $\Delta 4$ -desaturase (*Cr* $\Delta 4$ FAD) in *C. reinhardtii* that is involved

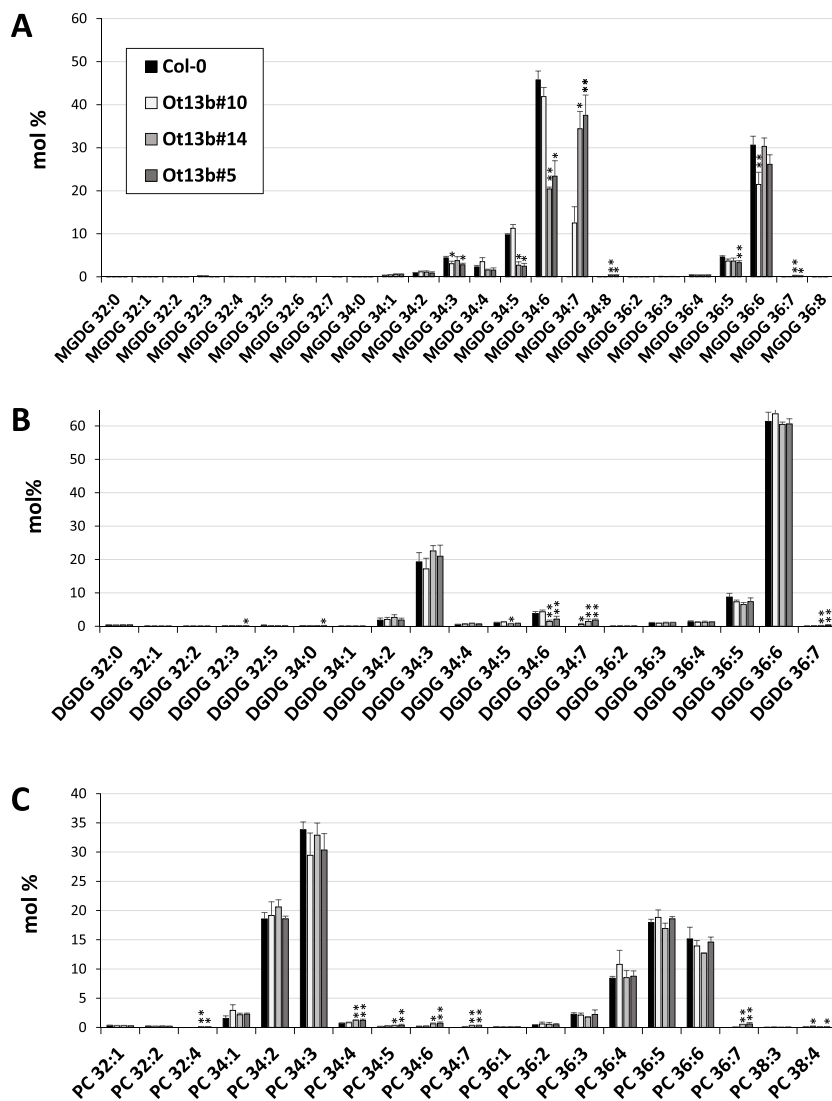


Fig. 5. Molecular profiling of major leaf glycerolipids from *Arabidopsis thaliana* lines overexpressing Ot13bDES and Col-0 control.

A: MGDG molecular species.

B: DGDG molecular species.

C: PC molecular species.

Lipid extracts were prepared from leaves of *Arabidopsis* lines expressing Ot13bDES under the control of the CaMV 35S promoter, and glycerolipids were analysed by LC-MS.

The data represent means \pm standard deviation of 4 biological replicates, and statistics were based on Kruskal-Wallis rank sum test with Dunn post-hoc analysis (*, 0.1- $p < 0.05$; **, 0.05- $p < 0.01$; *** $p < 0.001$).

in 16:4n3 biosynthesis. More recently, Degraeve-Guilbault et al. [26] functionally characterized the first two plastidial $\Delta 6$ -desaturases. These enzymes had no activity when expressed in the heterologous system *S. cerevisiae*, but using three different photosynthetic organisms, namely *N. benthamiana*, *Synechocystis*, and *O. tauri*, the authors could demonstrate their $\Delta 6$ desaturation activity on specific plastidic lipid species. Thus, in the present study, we report on the fourth plastidial front-end desaturase to be ever studied, and the first to be unambiguously characterized through heterologous expression as a front-end $\Delta 4$ -desaturase.

The heterologous expression experiments carried out in this work convincingly showed that Ot13bDES is a plastidial desaturase that converts 16:3n3 into 16:4n3, therefore displaying $\Delta 4$ -activity. The detailed lipidomic analyses of our best-performing *Arabidopsis* transgenic lines further showed a 16:3n3 conversion rate close to 100 %, indicating a very high catalytic activity. In

addition, our co-expression experiments with *O. tauri* plastidial $\Delta 6$ -desaturases (Ot05DES and/or Ot10DES) in *N. benthamiana* convincingly show that Ot13bDES has no $\Delta 3$ activity, and therefore suggest that Ot13bDES has a strict $\Delta 4$ -regioselectivity. While the detection of trace amounts of 18:4n3 in our best-performing Ot13bDES-overexpressing *Arabidopsis* lines may, in contrast, suggest that Ot13bDES displays a promiscuous $\Delta 6$ -activity towards 18:3n3, our preferred interpretation is that a yet-to-be-discovered plastidial elongating activity in *Arabidopsis* converts 16:4n3 into 18:4n3. The recent report of an elongation activity converting 16:1 $\Delta 7$ into 18:1 $\Delta 9$ in *Synechocystis* sp. PCC 6803 [45] supports the possibility that such activity may still be present in higher plants and could account for the low levels of 18:4n3 observed in our study. We also consider that the minor amounts of 16:4n3 detected in DGDG and PC most probably originate from the synthesis of these lipids from 16:4-containing MGDG (or deacylation/

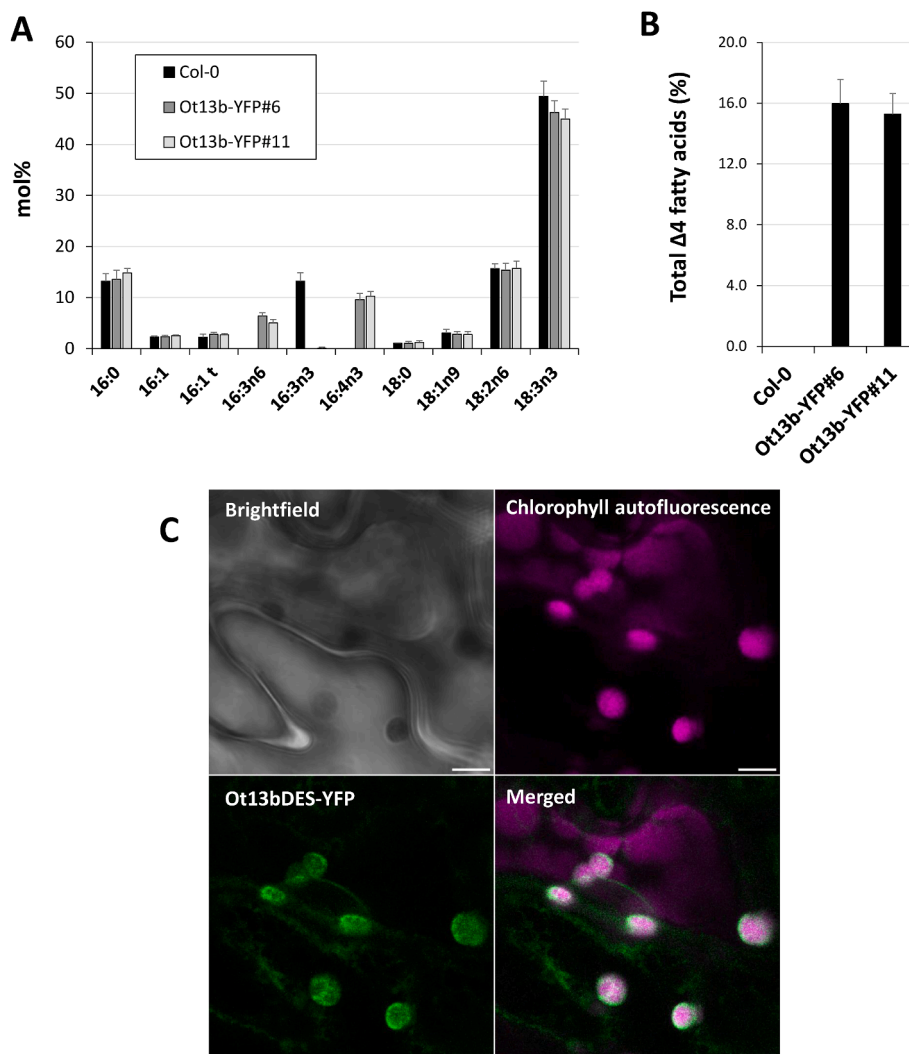


Fig. 6. Subcellular localization of Ot13bDES in Arabidopsis lines overexpressing Ot13bDES-YFP fusion protein.

A: Fatty acid composition of the different Arabidopsis lines overexpressing Ot13bDES-YFP fusion protein and Col-0 control.

B: Proportions of $\Delta 4$ -desaturated fatty acids in Arabidopsis lines overexpressing Ot13bDES-YFP fusion protein and Col-0 control.

C: Ot13bDES-YFP subcellular localization by confocal imaging (Bar = 5 μm).

Arabidopsis expressing Ot13bDES-YFP fusion protein under the control of the CaMV 35S promoter were generated and used for fatty acid analysis by GC and confocal imaging. The data represent means \pm standard deviation of 7–10 biological replicates, and statistics were based on Kruskal-Wallis rank sum test with Dunn post-hoc analysis (*, $0.1 < p < 0.05$; **, $0.05 < p < 0.01$; ***, $p < 0.001$).

reacylation of 16:4n3), rather than from Ot13bDES acting on these lipids. The distribution of 16:4n3 in our *A. thaliana* transgenic lines and *O. tauri* [26] could therefore further suggest that Ot13bDES displays a very strict specificity for lipid polar head group (i.e., MGDG) and the *sn*-position (i.e., *sn*-2) as previously reported for several microsomal front-end $\Delta 6$ -desaturases [46]. It is also possible that the very specific accumulation of 16:4n3 in Arabidopsis MGDG is due to the general nearly exclusive presence of 16:3n3 at the MGDG *sn*-2 position in higher plants. Nevertheless, the very specific regiolocalisation of 16:4n3 in *O. tauri* and in our transgenic lines strongly suggests that Ot13bDES is particularly active on the fatty acid present at the MGDG *sn*-2 position. *N. benthamiana* leaves are very rich in MGDG 36:6 (with 18:3n3 at both *sn*-positions; [37]), and *O. tauri* plastidial $\Delta 6$ -desaturases were shown to be highly efficient in converting 18:3n3 to 18:4n3 (particularly Ot05DES; [26]). We therefore speculate that in our coexpression experiments, 18:4n3 was produced at the *sn*-2 position of MGDG in *N. benthamiana*, but not further converted to

18:5n3, reinforcing the strict $\Delta 4$ -regioselectivity of Ot13bDES (no $\Delta 3$ -desaturation activity despite the presence of 18:4 at Ot13bDES's preferred MGDG *sn*-2 position). Finally, in the two heterologous expression systems we used (*N. benthamiana* and Arabidopsis), we observed the appearance of 16:4n3 as well as smaller amounts of 16:3n6. This may indicate that Ot13bDES requires the presence of a pre-existing $\Delta 7$ double bond in its substrate, as already suggested for Cr $\Delta 4$ FAD [22] and the microsomal $\Delta 4$ desaturase from *E. gracilis* [47].

In the present study, we also used yeast as a heterologous system to verify the activity of Ot01DES as a microsomal $\Delta 4$ -desaturase involved in DHA biosynthesis in *O. tauri*. In our phylogenetic tree, Ot01DES was highly similar to the functionally characterized microsomal $\Delta 4$ -desaturase from *O. lucimarinus* (Old4p; [28]), but also closely related to Ot13bDES. Ahmann et al. [28] previously demonstrated in yeast that Old4p actively desaturated supplemented 22:5n3 and 22:4n6, but also showed a low activity toward 16:3n3. Interestingly, *Old4p* was also co-expressed

with an MGDG synthase from *C. sativa* and supplied with 16:3n3. Although this strategy resulted in 16:3n3 incorporation into galactolipids, it did not increase the Old4p activity toward 16:3n3 [28]. Given that both Ot13bDES and Ot01DES possess PredAlgo-predicted chloroplast transit peptides [26], we used a similar approach to test whether Ot13bDES possesses microsomal $\Delta 4$ -desaturation activity. Contrary to Ot01DES, Ot13bDES showed no detectable conversion of 22:5n3 to 22:6n3, indicating that these enzymes are functionally different.

Our phylogenetic analysis showed that Ot13bDES clusters with the previously described Cr $\Delta 4$ FAD from *C. reinhardtii* [22]. Like Ot13bDES, Cr $\Delta 4$ FAD was shown to contain an N-terminal cytochrome *b5* domain and to be localized in the plastids of *C. reinhardtii*. Zäuner et al. [22] studied Cr $\Delta 4$ FAD through modulation of its expression in *C. reinhardtii* and reported that neither up- nor down-regulation affected MGDG 16:4n3 levels. However, their strategy modified the MGDG to DGDG ratio and consequently slightly impacted the total 16:4n3 and 18:3n3 levels. These findings highlighted a link between 16:4n3 availability and MGDG abundance and the predominant role of Cr $\Delta 4$ FAD in galactolipid homeostasis in *C. reinhardtii*. Nevertheless, Zäuner et al. [22] did not directly demonstrate the $\Delta 4$ -activity of Cr $\Delta 4$ FAD through heterologous expression. This strategy, usually performed in a host lacking the activity to be verified, is recommended for unambiguously determining the exact activity and regiospecificity of any putative front-end desaturase. The clear characterization of Ot13bDES as a plastidial $\Delta 4$ -desaturase in our study, along with its phylogenetic proximity with Cr $\Delta 4$ FAD, further supports that Cr $\Delta 4$ FAD has such an activity. Plastidic desaturases usually use ferredoxin and ferredoxin reductase as electron donors, while microsomal front-end desaturases use their N-terminal cytochrome *b5* domain and cytochrome *b5* reductase as electron donors. Zäuner et al. [22] showed through differences in spectral absorbance that the recombinant cytochrome *b5* domain of Cr $\Delta 4$ FAD was functional *in vitro*. Since, in addition, Yang et al. [48] reported physical interaction between ferredoxin 5 and Cr $\Delta 4$ FAD, it is highly probable that electron transfer occurs in these unusual plastidial front-end desaturases *via* ferredoxin and ferredoxin reductase through their N-terminal cytochrome *b5* domain.

Although both *C. reinhardtii* and *O. tauri* contain high levels of 16:4n3, the distribution of this peculiar fatty acid in these organisms clearly differs. In *C. reinhardtii*, 16:4n3 is mainly found in MGDG and nearly exclusively in galactolipids under optimal growth conditions [16]. In contrast, in *O. tauri*, this fatty acid is distributed across many different lipid classes, including plastidial MGDG and DGDG, microsomal DGTA and PDPT (which “replaces” PC in *O. tauri*), as well as DAG and TAG storage lipids. In addition, 16:4n3 accumulation in *C. reinhardtii* was shown to strongly depend on growth conditions, with nitrogen deprivation resulting in lower amounts [49]. Detailed lipidomic analyses have further shown that N-deprivation and heat stress resulted in the synthesis of 16:4n3-containing TAG from 16:4n3-containing MGDG (*via* DAG intermediates or a lipase/transacylase mechanism; [50,51]). Similarly, in *Chlorella* sp., 16:4n3 accumulation was shown to be reduced by heterotrophic or low-nutrient (nitrogen) conditions [52,53]. A similar trend was reported in *O. tauri*, although the overall picture was less clear since 16:4n3 is present in every class of *O. tauri* glycerolipids [19]. In particular, 16:4 is a major fatty acid of the extraplastidial lipid DGTA, where it occupies the *sn*-2 position, like in MGDG. However, in contrast, 16:4 was not detected in the *O. tauri*'s acyl-CoA pool, suggesting that MGDG-derived DAG might be exported from the chloroplasts to fuel the synthesis of 16:4n3-containing extraplastidial lipids. Another hypothesis is that Ot13bDES could be located at the chloroplast envelope, allowing it to modify both microsomal and plastidial lipid pools

[16,19]. However, both the precise suborganellar localization of Ot13bDES and the exact mechanism(s) behind *O. tauri* particular 16:4n3 distribution remain to be discovered.

In summary, we characterized in this study a plastidial front-end desaturase with $\Delta 4$ -regioselectivity involved in 16:4n3 biosynthesis in *O. tauri*. Stable expression in *A. thaliana* showed that the enzyme very efficiently converted all 16:3n3 into 16:4n3 without impacting plant development, suggesting that this rather novel type of desaturase may have a high biotechnological potential for the production of unusual fatty acids in plant biomass.

CRedit authorship contribution statement

M. Miklaszewska: Writing – review & editing, Writing – original draft, Investigation, Funding acquisition, Formal analysis, Data curation, Conceptualization. **R.E. Gomez:** Investigation, Data curation. **P. Van Delft:** Resources, Methodology. **M. Le Guédard:** Validation, Data curation. **C. Chambaud:** Methodology, Investigation. **C. Mirande-Bret:** Methodology, Investigation. **L. Fouillen:** Resources, Investigation, Data curation. **F. Corellou:** Writing – review & editing, Validation, Supervision, Project administration, Investigation, Funding acquisition, Conceptualization. **F. Domer-gue:** Writing – review & editing, Writing – original draft, Validation, Supervision, Project administration, Methodology, Investigation, Funding acquisition, Formal analysis, Data curation, Conceptualization.

Declaration of competing interest

Authors declare no conflicts of interest.
On the behalf of all co-authors.

Acknowledgements

This work was supported by the Centre National de la Recherche Scientifique and the University of Bordeaux. MM was supported by the French Government (BGF Scientific Research Stay Scholarship). Lipid analyses were carried out at the Metabolome facility of Bordeaux (<https://metabolome.u-bordeaux.fr/>). The Bordeaux Metabolome-Lipidome Facility-MetaboHUB is supported by a grant from ANR (no. ANR-11-INBS-0010).

Appendix A. Supplementary data

Supplementary data to this article can be found online at <https://doi.org/10.1016/j.biochi.2025.08.019>.

References

- [1] L. Tian, G. Chi, S. Lin, X. Ling, N. He, Marine microorganisms: natural factories for polyunsaturated fatty acid production, *Blue Biotechnology* 1 (2024) 15, <https://doi.org/10.1186/s44315-024-00012-8>.
- [2] K. Sun, D. Meesapyodsuk, X. Qiu, Molecular cloning and functional analysis of a plastidial $\omega 3$ desaturase from *Emiliana huxleyi*, *Front. Microbiol.* 15 (2024) 1381097, <https://doi.org/10.3389/fmicb.2024.1381097>.
- [3] J. Shanklin, E.B. Cahoon, Desaturation and related modifications of fatty acids, *Annu. Rev. Plant Physiol. Plant Mol. Biol.* 49 (1998) 611–641, <https://doi.org/10.1146/annurev.arplant.49.1.611>.
- [4] D. Meesapyodsuk, X. Qiu, The front-end desaturase: structure, function, evolution and biotechnological use, *Lipids* 47 (2012) 227–237, <https://doi.org/10.1007/s11745-011-3617-2>.
- [5] P. Sperling, P. Ternes, T.K. Zank, E. Heinz, The evolution of desaturases, *Prostagl. Leukot. Essent. Fat. Acids* 68 (2003) 73–95, [https://doi.org/10.1016/S0952-3278\(02\)00258-2](https://doi.org/10.1016/S0952-3278(02)00258-2).
- [6] B. Marin, M. Melkonian, Molecular phylogeny and classification of the Mamiellophyceae class. Nov. (chlorophyta) based on sequence comparisons of the nuclear- and plastid-encoded rRNA operons, *Protist* 161 (2010) 304–336, <https://doi.org/10.1016/j.protis.2009.10.002>.
- [7] X. Li, X. Fan, L. Han, Q. Lou, Fatty acids of some algae from the Bohai Sea, *Phytochemistry* 59 (2002) 157–161, [https://doi.org/10.1016/S0031-9422\(01](https://doi.org/10.1016/S0031-9422(01)

- 00437-X.
- [8] T. Takagi, M. Asahi, Y. Itabashi, Fatty acid composition of twelve algae from Japanese waters, *J. Jpn. Oil Chem. Soc.* 34 (1985) 1008–1012, <https://doi.org/10.5650/jos1956.34.1008>.
 - [9] A.-C. Viso, J.-C. Marty, Fatty acids from 28 marine microalgae, *Phytochemistry* 34 (1993) 1521–1533, [https://doi.org/10.1016/S0031-9422\(00\)90839-2](https://doi.org/10.1016/S0031-9422(00)90839-2).
 - [10] N.V. Zhukova, N.A. Aizdaicher, Fatty acid composition of 15 species of marine microalgae, *Phytochemistry* 39 (1995) 351–356, [https://doi.org/10.1016/0031-9422\(94\)00913-E](https://doi.org/10.1016/0031-9422(94)00913-E).
 - [11] S.H. Jónasdóttir, Fatty acid profiles and production in marine phytoplankton, *Mar. Drugs* 17 (2019) 151, <https://doi.org/10.3390/md17030151>.
 - [12] K. Ishihara, M. Murata, M. Kaneniwa, H. Saito, W. Komatsu, K. Shinohara, Purification of stearidonic acid (18:4(n-3)) and hexadecatetraenoic acid (16:4(n-3)) from algal fatty acid with lipase and medium pressure liquid chromatography, *Biosci. Biotechnol. Biochem.* 64 (2000) 2454–2457, <https://doi.org/10.1271/bbb.64.2454>.
 - [13] E.C.A. Stigter, S. Letsiou, N.J.F.V. Broek, J. Gerrits, K. Ishihara, E.E. Voest, N. M. Verhoeven-Duif, A.B. Brenkman, Development and validation of a quantitative LC–tandem MS assay for hexadeca-4,7,10,13-tetraenoic acid in human and mouse plasma, *J. Chromatogr. B* 925 (2013) 16–19, <https://doi.org/10.1016/j.jchromb.2013.01.012>.
 - [14] J. Schlotterbeck, A. Kolb, M. Lämmerhofer, Free fatty acid profiling in marine algae extract by LC-MS/MS and isolation as well as quantification of the ω -3 fatty acid hexadeca-4,7,10,13-tetraenoic acid, *J. of Separation Science* 41 (2018) 4286–4295, <https://doi.org/10.1002/jssc.201800780>.
 - [15] J.D. Leblond, B.E. Hollingsworth, D. Ayoub, M.B. McKinnon, C.S. Myers, T. J. Busari, K. Sabir, Galactolipid composition of the star-shaped dinoflagellate *Asterodinium gracile* (Kareniaceae): presence of hexadecatetraenoic acid (16:4(n-3))-containing monogalactosyldiacylglycerol as the predominant galactolipid and chemotaxonomic closeness to *Karenia mikimotoi* as the only other known Kareniacean producer of this fatty acid, *Phycol. Res.* 71 (2023) 135–139, <https://doi.org/10.1111/pre.12518>.
 - [16] Y. Li-Beisson, F. Beisson, W. Riekhof, Metabolism of acyl-lipids in *Chlamydomonas reinhardtii*, *Plant J.* 82 (2015) 504–522, <https://doi.org/10.1111/tpj.12787>.
 - [17] S. Shibata, S. Arimura, T. Ishikawa, K. Awai, Alterations of membrane lipid content correlated with chloroplast and mitochondria development in *Euglena gracilis*, *Front. Plant Sci.* 9 (2018) 370, <https://doi.org/10.3389/fpls.2018.00370>.
 - [18] C. Giroud, A. Gerber, W. Eichenberger, Lipids of *Chlamydomonas reinhardtii*. analysis of molecular species and intracellular site(s) of biosynthesis, *Plant Cell Physiol.* 29 (1988) 587–595, <https://doi.org/10.1093/oxfordjournals.pcp.a077533>.
 - [19] C. Degraeve-Guilbault, C. Bréhélin, R. Haslam, O. Sayanova, G. Marie-Luce, J. Jouhet, F. Corellou, Glycerolipid characterization and nutrient deprivation-associated changes in the green picoalga *Ostreococcus tauri*, *Plant Physiology* 173 (2017) 2060–2080, <https://doi.org/10.1104/pp.16.01467>.
 - [20] M. Siebertz, E. Heinz, Galactosylation of different monogalactosyldiacylglycerols by cell-free preparations from pea leaves, *Hoppe-Seyler's Zeitschrift Für Physiologische Chemie* 358 (1977) 27–34, <https://doi.org/10.1515/bchm2.1977.358.1.27>.
 - [21] I. Heilmann, M.S. Pidkowich, T. Girke, J. Shanklin, Switching desaturase enzyme specificity by alternate subcellular targeting, *Proc. Natl. Acad. Sci. USA* 101 (2004) 10266–10271, <https://doi.org/10.1073/pnas.0402200101>.
 - [22] S. Zäuner, W. Jochum, T. Bigorowski, C. Benning, A Cytochrome b_5 -Containing Plastid-located fatty acid desaturase from *Chlamydomonas reinhardtii*, *Eukaryot. Cell* 11 (2012) 856–863, <https://doi.org/10.1128/EC.00079-12>.
 - [23] C. De Los Reyes, J. Ávila-Román, M.J. Ortega, A. De La Jara, S. García-Mauriño, V. Motilva, E. Zubía, Oxylipins from the microalga *Chlamydomonas debarvana* and *Nannochloropsis gaditana* and their activity as TNF- α inhibitors, *Phytochemistry* 102 (2014) 152–161, <https://doi.org/10.1016/j.phytochem.2014.03.011>.
 - [24] H. Abida, L.-J. Dolch, C. Meï, V. Villanova, M. Conte, M.A. Block, G. Finazzi, O. Bastien, L. Tirichine, C. Bowler, F. Rébeillé, D. Petroutsos, J. Jouhet, E. Maréchal, Membrane glycerolipid remodeling triggered by nitrogen and phosphorus starvation in *Phaeodactylum tricornutum*, *Plant Physiol* 167 (2015) 118–136, <https://doi.org/10.1104/pp.114.252395>.
 - [25] L.-J. Dolch, E. Maréchal, Inventory of fatty acid desaturases in the pennate diatom *Phaeodactylum tricornutum*, *Mar. Drugs* 13 (2015) 1317–1339, <https://doi.org/10.3390/md13031317>.
 - [26] C. Degraeve-Guilbault, R.E. Gomez, C. Lemoigne, N. Pankasem, S. Morin, K. Tughile, J. Joubès, J. Jouhet, J. Gronnier, I. Suzuki, D. Coulon, F. Domergue, F. Corellou, Plastidic $\Delta 6$ fatty-acid desaturases with distinctive substrate specificity regulate the pool of c18-PUFAs in the ancestral picoalga *Ostreococcus tauri*, *Plant Physiol* 184 (2020) 82–96, <https://doi.org/10.1104/pp.20.00281>.
 - [27] F. Domergue, A. Abbadi, U. Zähringer, H. Moreau, E. Heinz, *In vivo* characterization of the first acyl-CoA $\Delta 6$ -desaturase from a member of the plant kingdom, the microalga *Ostreococcus tauri*, *Biochem. J.* 389 (2005) 483–490, <https://doi.org/10.1042/BJ20050111>.
 - [28] K. Ahmann, M. Heilmann, I. Feussner, Identification of a $\Delta 4$ -desaturase from the microalga *Ostreococcus lucimarinus*, *Eur. J. Lipid Sci. Technol.* 113 (2011) 832–840, <https://doi.org/10.1002/ejlt.201100069>.
 - [29] T. Ishikawa, F. Domergue, A. Amato, F. Corellou, Characterization of unique eukaryotic sphingolipids with temperature-dependent $\Delta 8$ -unsaturation from the picoalga *Ostreococcus tauri*, *Plant Cell Physiol.* 65 (2024) 1029–1046, <https://doi.org/10.1093/pcp/pcae007>.
 - [30] J. Joubès, S. Raffaele, B. Bourdenx, C. Garcia, J. Laroche-Traineau, P. Moreau, F. Domergue, R. Lessire, The VLCFA elongase gene family in *Arabidopsis thaliana*: phylogenetic analysis, 3D modelling and expression profiling, *Plant Mol. Biol.* 67 (2008) 547–566, <https://doi.org/10.1007/s11103-008-9339-z>.
 - [31] K. Tamura, G. Stecher, S. Kumar, MEGA11: molecular evolutionary genetics analysis version 11, *Mol. Biol. Evol.* 38 (2021) 3022–3027, <https://doi.org/10.1093/molbev/msab120>.
 - [32] D.T. Jones, W.R. Taylor, J.M. Thornton, The rapid generation of mutation data matrices from protein sequences, *Bioinformatics* 8 (1992) 275–282, <https://doi.org/10.1093/bioinformatics/8.3.275>.
 - [33] G.E. Crooks, G. Hon, J.-M. Chandonia, S.E. Brenner, WebLogo: a sequence logo generator: figure 1, *Genome Res.* 14 (2004) 1188–1190, <https://doi.org/10.1101/gr.849004>.
 - [34] R.J. Dohmen, A.W.M. Strasser, C.B. Höner, C.P. Hollenberg, An efficient transformation procedure enabling long-term storage of competent cells of various yeast genera, *Yeast* 7 (1991) 691–692, <https://doi.org/10.1002/yea.320070704>.
 - [35] S.J. Clough, A.F. Bent, Floral dip: a simplified method for agrobacterium-mediated transformation of *Arabidopsis thaliana*: floral dip transformation of *Arabidopsis*, *Plant J.* 16 (1998) 735–743, <https://doi.org/10.1046/j.1365-3113x.1998.00343.x>.
 - [36] M. Taridf, A. Atteia, M. Specht, G. Cogne, N. Rolland, S. Brugière, M. Hippler, M. Ferro, C. Bruley, G. Peltier, O. Vallon, L. Cournac, PredAlgo: a new sub-cellular localization prediction tool dedicated to green algae, *Mol. Biol. Evol.* 29 (2012) 3625–3639, <https://doi.org/10.1093/molbev/mss178>.
 - [37] S. Okada, M. Taylor, X.-R. Zhou, F. Naim, D. Marshall, S.J. Blanksby, S.P. Singh, C.C. Wood, Producing cyclopropane fatty acid in plant leafy biomass via expression of bacterial and plant cyclopropane fatty acid synthases, *Front. Plant Sci.* 11 (2020), <https://doi.org/10.3389/fpls.2020.00030>.
 - [38] S. Li, D.W. Ehrhardt, S.Y. Rhee, Systematic analysis of *Arabidopsis* organelles and a protein localization database for facilitating fluorescent tagging of full-length *Arabidopsis* proteins, *Plant Physiol* 141 (2006) 527–539, <https://doi.org/10.1104/pp.106.078881>.
 - [39] E.B. Cahoon, A.M. Cranmer, J. Shanklin, J.B. Ohlrogge, $\Delta 6$ hexadecenoic acid is synthesized by the activity of a soluble $\Delta 6$ palmitoyl-acyl carrier protein desaturase in *Thunbergia alata* endosperm, *J. Biol. Chem.* 269 (1994) 27519–27526.
 - [40] X. Qiu, H. Hong, S.L. MacKenzie, Identification of a $\Delta 4$ fatty acid desaturase from *Thraustochytrium sp.* involved in the biosynthesis of docosahexaenoic acid by heterologous expression in *Saccharomyces cerevisiae* and *Brassica juncea*, *J. Biol. Chem.* 276 (2001) 31561–31566, <https://doi.org/10.1074/jbc.M102971200>.
 - [41] A. Oboh, N. Kabeya, G. Carmona-Antoñanzas, L.F.C. Castro, J.R. Dick, D. R. Tocher, O. Monroig, Two alternative pathways for docosahexaenoic acid (DHA, 22:6n-3) biosynthesis are widespread among teleost fish, *Sci. Rep.* 7 (2017) 3889, <https://doi.org/10.1038/s41598-017-04288-2>.
 - [42] P. Ternes, S. Franke, U. Zähringer, P. Sperling, E. Heinz, Identification and Characterization of a sphingolipid $\Delta 4$ -desaturase family, *J. Biol. Chem.* 277 (2002) 25512–25518, <https://doi.org/10.1074/jbc.M202947200>.
 - [43] L.V. Michaelson, S. Zäuner, J.E. Markham, R.P. Haslam, R. Desikan, S. Mugford, S. Albrecht, D. Warnecke, P. Sperling, E. Heinz, J.A. Napier, Functional characterization of a higher plant sphingolipid $\Delta 4$ -desaturase: defining the role of sphingosine and sphingosine-1-phosphate in *Arabidopsis*, *Plant Physiology* 149 (2009) 487–498, <https://doi.org/10.1104/pp.108.129411>.
 - [44] Y. Bai, J.G. McCoy, E.J. Levin, P. Sobrado, K.R. Rajashankar, B.G. Fox, M. Zhou, X-ray structure of a mammalian stearyl-CoA desaturase, *Nature* 524 (2015) 252–256, <https://doi.org/10.1038/nature14549>.
 - [45] A. Kobayashi, N. Pankasem, K. Kobayashi, F. Corellou, K. Yoneda, Y. Maeda, I. Suzuki, Cold-sensitive pathway elongates a non-native cis-7-hexadecenoic acid to cis-9-octadecenoic acid in the cyanobacterium *Synechocystis sp.* PCC 6803, *Biochim. Biophys. Acta Mol. Cell Biol. Lipids* 1870 (2025) 159649, <https://doi.org/10.1016/j.bbalip.2025.159649>.
 - [46] F. Domergue, A. Abbadi, C. Ott, T.K. Zank, U. Zähringer, E. Heinz, Acyl carriers used as substrates by the desaturases and elongases involved in very long-chain polyunsaturated fatty acids biosynthesis reconstituted in yeast, *J. Biol. Chem.* 278 (2003) 35115–35126, <https://doi.org/10.1074/jbc.M305990200>.
 - [47] A. Meyer, P. Cirpus, C. Ott, R. Schlecker, U. Zähringer, E. Heinz, Biosynthesis of docosahexaenoic acid in *Euglena gracilis*: biochemical and molecular evidence for the involvement of the desaturases and elongases, *Biochemistry* 42 (2003) 9779–9788, <https://doi.org/10.1021/bi034731y>.
 - [48] W. Yang, T.M. Wittkopp, X. Li, J. Warakanont, A. Dubini, C. Catalanotti, R. G. Kim, E.C.M. Nowack, L.C.M. Mackinder, M. Aksoy, M.D. Page, S. D'Adamo, S. Saroussi, M. Heinnickel, X. Johnson, P. Richaud, J. Alric, M. Boehm, M. C. Jonikas, C. Benning, S.S. Merchant, M.C. Posewitz, A.R. Grossman, Critical role of *Chlamydomonas reinhardtii* ferredoxin-5 in maintaining membrane structure and dark metabolism, *Proc. Natl. Acad. Sci. USA* 112 (2015) 14978–14983, <https://doi.org/10.1073/pnas.1515240112>.
 - [49] R.T. Smith, D.J. Gilmour, The influence of exogenous organic carbon assimilation and photoperiod on the carbon and lipid metabolism of *Chlamydomonas reinhardtii*, *Algal Res.* 31 (2018) 122–137, <https://doi.org/10.1016/j.algal.2018.01.020>.
 - [50] B. Légeret, M. Schulz-Raffelt, H.M. Nguyen, P. Auroy, F. Beisson, G. Peltier,

- G. Blanc, Y. Li-Beisson, Lipidomic and transcriptomic analyses of *Chlamydomonas reinhardtii* under heat stress unveil a direct route for the conversion of membrane lipids into storage lipids: lipid remodelling under heat stress in *chlamydomonas*, *Plant Cell Environ.* 39 (2016) 834–847, <https://doi.org/10.1111/pce.12656>.
- [51] D.Y. Young, Y. Shachar-Hill, Large fluxes of fatty acids from membranes to triacylglycerol and back during N-deprivation and recovery in *Chlamydomonas*, *Plant Physiology* 185 (2021) 796–814, <https://doi.org/10.1093/plphys/kiab071>.
- [52] L.G. Dickson, R.A. Galloway, G.W. Patterson, Environmentally-induced changes in the fatty acids of *chlorella*, *Plant Physiol* 44 (1969) 1413–1416, <https://doi.org/10.1104/pp.44.10.1413>.
- [53] D.A. White, P.A. Rooks, S. Kimmance, K. Tait, M. Jones, G.A. Tarran, C. Cook, C. A. Llewellyn, Modulation of polar lipid profiles in *chlorella* sp. in response to nutrient limitation, *Metabolites* 9 (2019) 39, <https://doi.org/10.3390/metabo9030039>.